

A SIMPLE MULTIPLE SCATTERING – DEPOLARIZATION RELATION OF WATER CLOUDS AND ITS POTENTIAL APPLICATIONS

Yongxiang Hu⁽¹⁾, Mark A. Vaughan⁽¹⁾, David M. Winker⁽¹⁾, Zhaoyang Liu⁽¹⁾, Vincent Noel⁽⁴⁾,
Luc R. Bissonnette⁽²⁾, Gilles Roy⁽²⁾, Matthew McGill⁽³⁾, Charles R. Trepte⁽¹⁾

⁽¹⁾ MS 475, NASA Langley Research Center, Hampton, VA 23681, USA, yongxiang.hu-1@nasa.gov

⁽²⁾ RDDC Valcartier, Val-Belair, QC G3J 1X5, Canada, Luc.Bissonnette@drdc-rddc.gc.ca

⁽³⁾ Code 613.1, NASA Goddard Space Flight Center, Greenbelt, MD 20771, USA, Matthew.J.McGill@nasa.gov

⁽⁴⁾ Laboratoire de Météorologie Dynamique, Ecole Polytechnique, Palaiseau, France, vincent.noel@lmd.polytechnique.fr

ABSTRACT

An empirical relationship is derived between multiple scattering fraction and linear depolarization ratio using Monte Carlo simulations of water clouds measured by backscatter lidar. This relationship is shown to hold for water clouds with a wide range of extinction coefficients, mean droplet sizes, and droplet size distribution widths. The relationship is also shown to persist for various instrument fields-of-view, and for measurements made within broken cloud fields. The results obtained from the Monte Carlo simulations are verified using multiple fields-of-view lidar measurements. For space-based lidars equipped to measure linear depolarization ratios, this new relationship can be used to accurately assess signal perturbations due to multiple scattering and to estimate the integrated single scattering returns within non-precipitating water clouds. By applying this simple relation, we can calibrate space-based lidar using water clouds to an accuracy of about 2% for 532 nm and 3% for 1064 nm. Other applications include measuring column optical depths of thin clouds and aerosols above the water clouds and oriented plate – water cloud discrimination.

1. A SIMPLE RELATION BETWEEN MULTIPLE SCATTERING AND DEPOLARIZATION OF WATER CLOUDS

With their well-behaved single scattering properties and strong backscatter signal, water clouds could be good targets for validations of lidar measurements. Due to the very small mean free path for photon scattering typical of water clouds, lidar backscatter measurements will always contain contributions from multiple scattering, and thus affect lidar data analysis. We introduce a polynomial approximation, derived via Monte Carlo simulations, that provides a highly accurate description of the relationship between the linear depolarization of backscatter signal and the fraction of multiple scattering present in the signal. The validity of the relationship is demonstrated using multiple-field-of-view (MFOV) lidar backscatter measurements made using the Defense R&D Canada Valcartier (DRDC-V) lidar [1]. This relation makes possible the correction of multiple scattering effects and the reliable retrieval of single-scattering optical properties

from water cloud lidar measurements with linear depolarization ratios [2].

Single scattering from spherical droplets in the 180° backscatter direction retains the polarization of the incident light, but scattering at other scattering angle alters the polarization state. Thus, for a lidar transmitting a linearly polarized beam, the single backscatter signal from a water cloud is also linearly polarized, and depolarization of the signal can be attributed to multiple scattering effects [3]. To investigate the relation between multiple scattering and depolarization ratios we define two scattering parameters. We term the first one the “accumulated single scattering fraction”, $A_s(r)$, such that

$$A_s(r) = I_s(r) / I_T(r). \quad (1)$$

$$\text{where } I_s(r) = \int_{r_0}^r X_s(r') dr' \quad \text{and} \quad I_T(r) = \int_{r_0}^r X_T(r') dr'$$

are, respectively, the integrated, range-corrected single-scattering (X_s) and total-scattering ($X_T = \text{single} + \text{multiple}$) lidar backscatter signals computed over the range r_0 to r , where r_0 is the near-range boundary of the cloud being measured (i.e., $r_0 = \text{cloud base}$ for up-looking systems, and cloud top for down-looking lidars). Similarly, we also define the “accumulated depolarization ratio”, $\delta_{acc}(r)$, such that

$$\delta_{acc}(r) = I_{T,\perp}(r) / I_{T,\parallel}(r) \quad (2)$$

and $I_{T,\parallel}(r)$ and $I_{T,\perp}(r)$ represent, respectively, the components of the total backscattered signal, X_T , polarized parallel (\parallel) and perpendicular (\perp) to the polarization plane of the laser transmitter; that is,

$$I_{T,\parallel}(r) = \int_{r_0}^r X_{T,\parallel}(r') dr' \quad \text{and} \quad I_{T,\perp}(r) = \int_{r_0}^r X_{T,\perp}(r') dr'.$$

The relationship between δ_{acc} and A_s was investigated via a Monte Carlo study that examined simulated lidar backscatter signals derived from a number of different water cloud models.

A standard Mie scattering code [4] was used to compute the single-scattering matrices for non-precipitating (spherical) water cloud droplets. These in turn provided the necessary inputs for the full-Stokes vector Monte

Carlo code [5] that was used to generate the simulated multiple-scattering signals. Special care was given to deriving the correct rotation angles between different reference planes when $\sin\Theta$, $\sin\theta_0$, or $\sin\theta_1$ becomes zero.

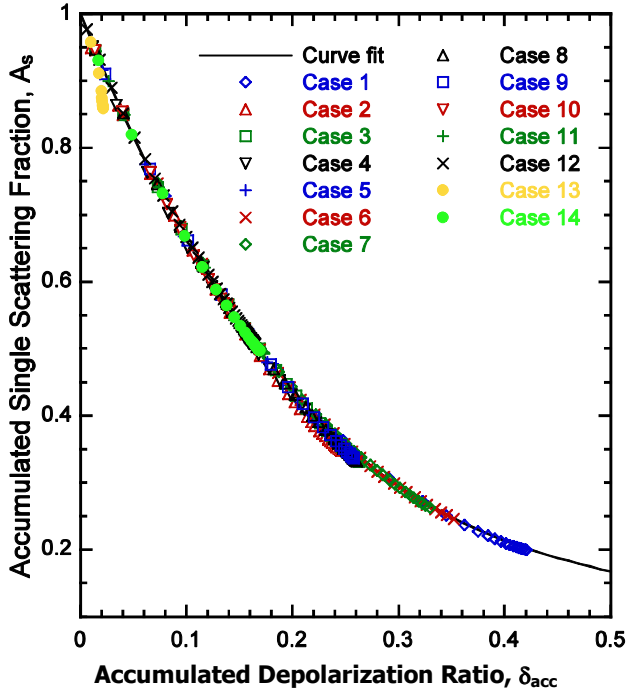


Fig. 1. Relation between A_s and δ_{acc} . The relation is valid for a variety of extinction coefficients, particle size distributions, cloud geometries, and lidar fields-of-view.

To ensure a thorough examination of the underlying physics, hundreds of measurement scenarios were modeled. These scenarios include a diverse set of cloud physical and optical properties, combined with a number of different lidar fields-of-view (FOVs). The individual test cases were selected to encompass the widest possible variety of realistic measurement conditions. The water clouds were parameterized using extinction coefficients ($\sigma = 1 \text{ km}^{-1}$ to 100 km^{-1}) and effective radii ($Re = 4 \text{ }\mu\text{m}$ to $12 \text{ }\mu\text{m}$), and the widths of the (assumed) Gamma distribution for droplet sizes ($\gamma = 3$ to 25). The gamma distribution is used throughout this study as it has been shown to provide a realistic representation of the actual droplet size distributions in water clouds [6]. Broken clouds are also considered. Because the amount of multiple scattering present in the lidar backscatter signal depends strongly on the receiver's FOV, this parameter was also varied (FOV = 0.04 to 1.3 mrad for space-based lidar) within the simulation. The geometric thickness of the modeled clouds ranged between 0.2 km and 1 km. The space-based lidar is assumed to have a range to the cloud of 700 km. Simulations were also performed on ground-based measurements (cloud base height 0.7 km) with FOV up to 16 mrad. All simulations were conducted using laser wavelengths of 532 nm and 1064 nm.

A plot of representative $A_s(r)$ and $\delta_{acc}(r)$ values derived from the simulations is shown in Fig. 1. The individual symbols represent the results obtained for 14 separate cases from among the complete set of simulation results. In each of these cases, the simulation from which the $A_s(r)$ and $\delta_{acc}(r)$ values were computed used a different combination of extinction coefficient (σ), mean particle size (Re), Gamma size distribution width (γ), and lidar FOV. Also included among the example cases are two instances of broken clouds (see cases 8 and 9, for which the cloud fraction is less than 1.0) and 5 cases of ground-based lidar (see case 9 to 14). The exact parameterizations used for each case are listed in Table 1.

Table 1: model parameters for the simulation results shown in Fig. 1

Case	λ (nm)	Gr. /Sp.	Re μm	γ	τ	FOV mrad	Cloud Frac.
1	532	Space	4	6	20	0.13	1.0
2	532	Space	8	16	8	0.13	1.0
3	532	Space	8	6	8	0.13	1.0
4	1064	Space	8	6	8	0.13	1.0
5	1064	Space	4	25	8	0.13	1.0
6	532	Space	4	6	8	1.3	1.0
7	532	Space	4	6	8	0.04	1.0
8	532	Space	4	6	8	0.13	0.5
9	532	Space	4	6	8	0.13	0.3
10	1064	Ground	4	6	8	12	1.0
11	532	Ground	8	6	16	12	1.0
12	532	Ground	3	6	10	16	1.0
13	532	Ground	8	6	16	0.5	1.0
14	1064	Ground	4	6	8	6	1.0

Examining the 14 cases shown in Fig. 1 (each is plotted using a unique symbol and multiple points for each case are for different ranges into the cloud layer), it is obvious there is a simple relation between the accumulated single scattering fraction, $A_s(r)$, and the accumulated depolarization ratio, $\delta_{acc}(r)$. The solid line represents a 3rd-order polynomial least-squares fit to the entire set of $A_s(r)$ and $\delta_{acc}(r)$ data pairs derived from all of the simulations. The good agreement between these examples and the least-squares fit is shared by all of the space-based lidar cases simulated, regardless of cloud microphysics, macrophysics, and lidar FOV. For $\delta_{acc} < 0.5$, the exact functional relationship between the two scattering parameters is given by

$$A_s = 0.999 - 3.906 \delta_{acc} + 6.263 \delta_{acc}^2 - 3.554 \delta_{acc}^3. \quad (3)$$

By applying Eq. (3) to the lidar backscatter profiles generated in this simulation study, the multiple scattering contributions to the signals can be estimated and removed

with the smoothly varying water cloud depolarization data. When the single scattering approximations derived using Eq. (3) are compared to the “known truth” record for each simulation, the corrected profiles are found to be within 2% of the true values for all space-based lidar cases and most ground-based lidar cases with relatively large FOV. In these cases, lower-order multiple scattering in all scattering angles are within the FOV. Eq. (3) is less accurate for ground-based lidar cases with footprint sizes less than 3 m and with small extinction coefficients, when multiple scattering is mostly scattering in forward and backward directions.

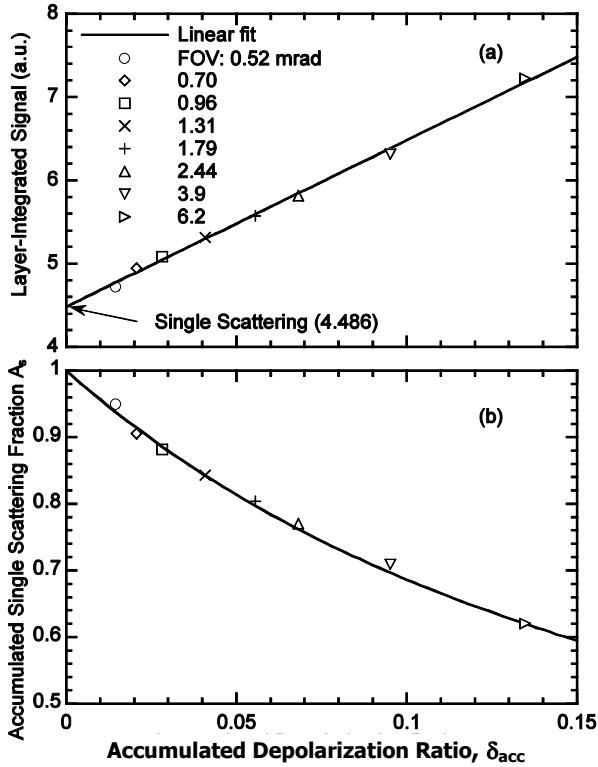


Fig. 2. Upper panel: deriving single scattering component from the MFOV lidar observations through extrapolations. Lower panel: the comparison between the eight field-of-view lidar observations with the $A_s - \delta_{acc}$ relation of Eq. (3). A_s is computed using 4.488 from the upper panel divided by MFOV measurements. Although the observed relationship between $A_s(r)$ and $\delta_{acc}(r)$ agrees well with Eq. (3) at all cloud penetration depths, only integrals of A_s and δ_{acc} through the entire cloud layer are plotted.

2. VALIDATING THE SIMPLE RELATION WITH MFOV LIDAR MEASUREMENTS

Validation of Eq. (3) was accomplished using field measurements of water clouds acquired by the MFOV lidar on 6 December 1999, during the Alliance Icing Research Study (AIRS) experiment in Canada [7]. The Defense R&D Canada (DRDV) lidar has eight concentric fields-of-view at 0.52, 0.7, 0.96, 1.31, 1.79, 2.44, 3.9, and

6.2 mrad, and can measure linear depolarization ratio at 1064 nm for each FOV channel. Both A_s and δ_{acc} can be obtained from DRDC-V measurements. A plot of the layer integrated backscatter as a function of the layer integrated depolarization ratio, δ_{acc} (which can be derived directly), is shown in Fig. 2(a) for all eight FOV channels. As the relationship can be approximated using a linear fit, we estimate the layer integrated single-scattering signal, $I_s(r)$, by extrapolating the MFOV integrated lidar backscatter signals to $\delta_{acc}=0$. The value obtained by this method (4.488, arbitrary unit) is then used to derive the single-scattering fractions (A_s) for all FOVs. The resulting single-scattering fraction values, computed by integrating over the entire cloud layer, are shown in Fig. 2(b), again as a function of corresponding integrated depolarization ratio. The values computed from the lidar measurements are shown using symbols. Also shown (using a solid line) are the approximations to A_s computed using Eq. 3. Examination of the figure shows that the predicted values derived using the polynomial approximation agree quite well with the lidar observations.

3. APPLICATIONS OF THE SIMPLE RELATION FOR CALIBRATION OF SPACE-BASED LIDARS

By applying this simple relation between multiple scattering and depolarization of water clouds to measured data, a number of useful properties can be derived. Among the most important of these is the calibration and/or validation of space-based lidar systems, which is obtained by comparing the integrated attenuated signals of optically thick water clouds (e.g., cloud optical depth $> \sim 3$) with the theoretical limit of $1/(2S_c)$, where S_c is the extinction-to-backscatter ratio [8]. Using A_s for multiple scattering removals, the calibration is derived as follows:

$$\frac{A_s}{C} \sum_{j=top}^{base} r_j^2 P(r_j) = \int_{r_{top}}^{r_{base}} \frac{e^{-2\tau(r)}}{S_c} d\tau(r) = \frac{1 - e^{-2\tau_c}}{2S_c} \quad (4)$$

where $P(r)$ is the range-resolved backscatter signal from a dense water cloud, and C is the lidar calibration constant.

When the cloud optical depth is large, $e^{-2\tau_c} \approx 0$, thus

$$C \approx 2A_s S_c \sum_{j=top}^{base} r_j^2 P(r_j) \quad (5)$$

This approach requires knowledge of the single scattering factor, A_s , derived from Eq. (3), and the lidar ratio, S_c . The performance of the method therefore depends on how accurately we know (or can estimate) A_s and S_c . Given accurate depolarization ratios measurements, A_s can be retrieved accurately using Eq. (3). For water clouds, S_c is known to have a relatively stable value at the visible and near infrared wavelengths [9,10]. However, previously reported uncertainties [9] associated with S_c are relatively large for water clouds occurring over land.

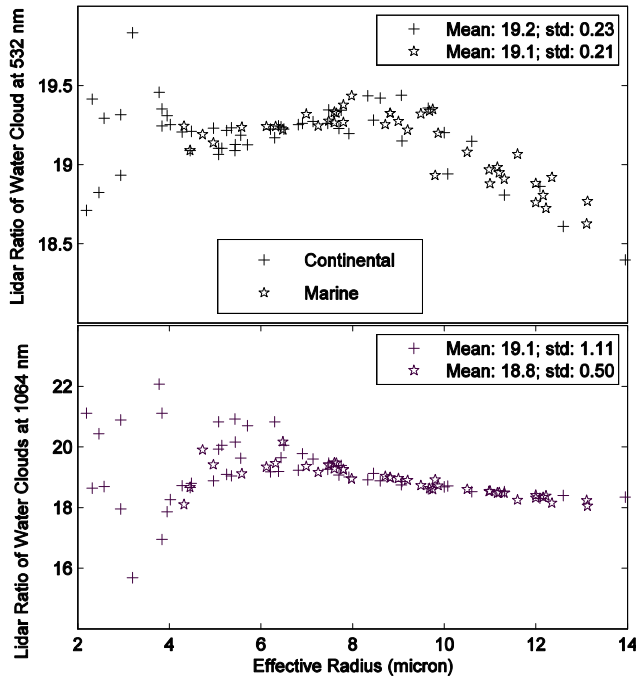


Fig. 3. Extinction-to-backscatter ratios (S_c) calculated using the widths and mode-radii from all historical water cloud particle size distribution observations [6].

To make the calibration technique viable, two questions need to be answered: how well can we estimate S_c , and what type of water clouds should be used for space-based calibrations? Since S_c is known to vary according to cloud droplet size distribution, the answer requires an in-depth knowledge of water cloud droplet size distributions, preferably obtained from in situ measurements. Miles et al. [6] provide a complete listing of water cloud size distributions, compiled from all available in situ measurements. This list includes 41 distributions for water clouds over ocean and 51 distributions for water clouds over land. In each case, the measured data are fitted with Gamma distributions. Using these water cloud droplet size distributions, we have computed values for S_c using exact Mie theory with half a million size-bins between 1 and 50 μm . Each S_c data point in Fig. 3 corresponds to a calculation derived from one size distribution.

Fig. 3 suggests that we should choose water clouds over ocean as the targets for calibration since the uncertainty of S_c for water clouds over ocean (1% at 532 nm and 2.5% at 1064 nm) is smaller than that of the water clouds over land (1.2% at 532 nm and 6% at 1064 nm). Using a parameterized backscatter-size parameter relation, Pinnick et al. estimated that the uncertainty in S_c is $\sim 10\%$ at 1064 nm for water clouds observed over land [9]. As a result of using more representative and complete size distributions, and the improved computational capability of modern digital computers, Fig. 3 shows that the uncertainty of S_c is less than Pinnick's estimation, espe-

cially for water clouds over ocean and for 532 nm channel. In addition, both A_s and S_c can be more accurately estimated with effective droplet radii derived from CALIPSO IIR or MODIS, and thus lead to further improvement in the performance of this calibration technique.

4. SUMMARY AND OTHER APPLICATIONS

A simple, empirical relationship is derived between multiple scattering and linear depolarization ratio using Monte Carlo simulations of water clouds measured by backscatter lidar. This relationship is shown to hold for water clouds with a wide range of extinction coefficients, mean droplet sizes, and drop size distribution widths. This relationship, together with the stable water cloud lidar ratios, provides accurate lidar calibrations for both 532 nm and 1064 nm.

Alternately, if the lidar is already well calibrated, total column optical depth of thin clouds and/or aerosols above the water cloud layer can be accurately estimated. This simple relation can also be applied to help discriminate between water cloud and oriented ice plate particles.

REFERENCES

1. Bissonnette L.R. et al. Range-height scans of lidar depolarization for characterizing properties, *J. A. O. Tech.*, **18**, 1429-1446, 2001.
2. Sassen K., The Polarization Lidar Technique for Cloud Research: A Review and Current Assessment, *Bull. Am. Meteorol. Soc.*, **72**, pp. 1848-1866, 1991.
3. Sassen K. and Pettrilla R.L., Lidar depolarization from multiple scattering in marine stratus clouds, *Appl. Opt.*, **25**, 1450-1459, 1986.
4. Wiscombe W., Improved Mie scattering algorithms, *Appl. Opt.*, **19**, 1505-1509, 1980.
5. Hu Y., et al. Identification of cloud phase from PICASSO-CENA lidar depolarization. *J.Q.S.R.T.*, **70**, 569-579, 2001.
6. Miles N.J., et al. Cloud droplet size distributions in low-level stratiform clouds, *J. Atmos. Sci.*, **57**, 295-311, 2000.
7. Bissonnette L.R., et al. Multiple-scattering lidar retrieval method, *Appl. Optics*, **41**, 6307-6324, 2002.
8. Platt M., et al., Backscatter-to-Extinction Ratios in the Top Layers of Tropical Mesoscale Convective Systems and in Isolated Cirrus from LITE Observations. *J. App. Meteor.*, **38**, 1330-1345, 1999.
9. Pinnick R.G., et al. Backscatter and Extinction in Water Clouds, *J.G.R.*, **88**, 6787-6796, 1983.
10. O'Connor E.J., et al. A technique for auto-calibration of cloud lidar, *J. Atmos. Oc. T.*, **21**, 777-786, 2004.